APPLICATION OF THE MASTER CURVE METHODOLOGY TO FRACTURE TOUGHNESS CHARACTERIZATION OF FERRITIC-MARTENSITIC STEEL

M.A.Sokolov[1] and H. Tanigawa[2]
[1] Metals and Ceramics Division, Oak Ridge National Laboratory, Oak Ridge, TN 37831, USA
[2] Japan Atomic Energy Research Institute, Tokai, Ibaraki, 319-1195, JAPAN

ABSTRACT

Recent advances in fracture toughness have led to employment of the Weibull statistic to model scatter of fracture toughness in the transition region of low-alloyed ferritic steels. This methodology uses a concept of the universal temperature dependence of fracture toughness in the transition region, the so-called "master curve". The current physical background for this methodology suggests that it is applicable to a wide variety of ferritic bcc steels, including tempered ferritic-martensitic steels. Those steels are structural material candidates for fusion reactors. However, irradiation embrittlement (shift of the ductile-to-brittle transition region) of these steels is one of the main concerns for application purposes. Yet, the transition fracture toughness data for this class of steels are rather sparse. In this study, two types of fracture toughness specimens of a F82H steel were tested to verify the master curve concept. Specimens were tested at several temperatures in the transition region and at least four specimens were tested at each temperature allowing for application of the Weibull statistic/master curve analysis procedure. The largest specimens were 1T compact specimens. Broken halves of 1T specimens were later used to machine and test smaller, 0.4T, size specimens which could be more suitable for irradiation experiments. It was shown that scatter of fracture toughness of this material was rather high relative to scatter of low-alloyed steels but it was similar between larger and smaller specimens.

1 INTRODUCTION

The reduced-activation ferritic-martensitic (RAFM) steel F82H is a primary candidate low-activation material for fusion applications, and it is being investigated in the joint U.S. Department of Energy-Japan Atomic Energy Research Institute (DOE-JAERI) collaboration program. The F82H alloy (Fe-8Cr-2W-V-Ta) was developed by JAERI and NKK Corporation, Kawasaki, Japan and provided world-wide for the International Energy Agency (IEA) round-robin tests. Material used for the IEA round robin tests was melted in two 5 metric-ton heats (heat #9741 and #9753). 7.5-mm thickness plates, and 15-mm thickness plates, were produced from heat #9741 and the 15mm thickness plates and 25mm thickness plates were produced from heat #9753. All 1T-CT fracture toughness specimens were taken from 25-mm thickness plates from heat No.9753. 25-mm thickness plates were distributed in two conditions. One condition was standard heat treatment, and the other was TIG-welded or EB-welded followed by post weld heat treatment (PWHT).

In this study, fracture toughness of 25-mm-thick plate from heat #9753 that underwent PWHT after TIG welding has been characterized in the transition region by testing 1T and 0.4T C(T) specimens. All specimens were machined in the L-T orientation such that the crack would propagate in the transverse orientation.

2 TESTING PROCEDURE

The fracture toughness tests were conducted in general accordance with the ASTM E 1921-02 Standard Test Method for Determination of Reference Temperature, T_o, for Ferritic Steels in the

Transition Range, with a computer-controlled test and data acquisition system (Nanstad [1]). The specimens were fatigue precracked before irradiation to a ratio of the crack length to specimen width (a/W) of about 0.5, and then side-grooved by 20% of their thickness (10% from each side). The unloading compliance method was used for measuring ductile crack growth. Specimens were tested in the laboratory on a 98-kN (22-kip) capacity servohydraulic machine. All tests were conducted in strain control, with an outboard clip gage having a central flexural beam that was instrumented with four strain gages in a full-bridge configuration. The broken specimens were examined with a calibrated measuring optical microscope to determine the initial and final crack lengths.

3 ANALYSIS PROCEDURE

Values of J-integral at cleavage instability, J_c, were converted to their equivalent values in terms of stress intensity factor K_{Jc} by the following equation:

$$K_{Jc} = \sqrt{J_c \frac{E}{1-\nu^2}} \tag{1}$$

where E is Young's modulus and ν=0.3 is Poisson's ratio.

All K_{Jc} data were converted to 1T equivalence, $K_{Jc(1T)}$, using the size adjustment procedure of E1921:

$$K_{Jc(1T)} = 20 + \left[K_{Jc(xT)} - 20\right]\left(\frac{B_{xT}}{B_{1T}}\right)^{1/4} \tag{2}$$

where $K_{Jc(xT)}$ = measured K_{Jc} value, B_{xT} = gross thickness of test specimen, B_{1T} = gross thickness of 1T C(T) specimen.

The reference fracture toughness transition temperature, T_o, was determined using the multi-temperature equation from E1921:

$$\sum_{i=1}^{N} \delta_i \frac{\exp[0.019(T_i - T_o)]}{11 + 77\exp[0.019(T_i - T_o)]} - \sum_{i=1}^{N} \frac{\left(K_{Jc(i)} - 20\right)^4 \exp[0.019(T_i - T_o)]}{\{11 + 77\exp[0.019(T_i - T_o)]\}^5} = 0 \tag{3}$$

where δ_i= 1.0 if the datum is valid or zero if datum is a dummy substitute value, T_i= test temperature corresponding to $K_{Jc(i)}$.

The K_{Jc} value was considered invalid if it exceeded the validity limit:

$$K_{Jc(limit)} = \sqrt{\frac{E b_o \sigma_{YS}}{30(1-\nu^2)}} \tag{4}$$

where b_o is the in-plane size of the remaining ligament of the specimen and σ_{ys} is yield strength of material. If the measured value exceeded the validity limit, it was considered an invalid value and replaced with the $K_{Jc\,(limit)}$ value for T_o calculation.

4 TEST RESULTS AND DISCUSSION

A total of 46 specimens have been tested in the transition region, 27 1T C(T) and 19 0.4T C(T). One 0.4T compact specimen tested at -20°C did not cleave. The test was stopped because the clip gage ran out of measuring range. Final the J-integral value at the end of the test was higher than $K_{Jc\,(limit)}$ value; thus it was treated as an invalid specimen. The reference fracture toughness transition temperature, T_o, for this data set is determined to be equal to -102°C. Figure 1 illustrates the 1T size-adjusted fracture toughness data vs test temperature, with the master curve and the 5% and 95% tolerance bounds from this analysis added.

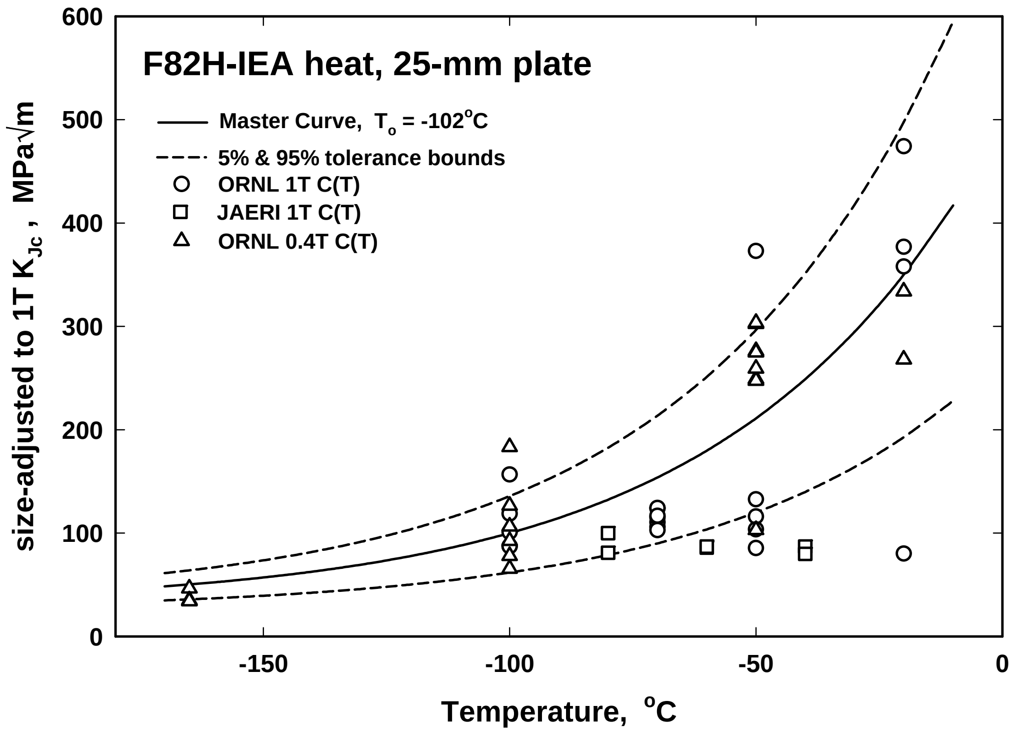

Figure 1: Size-adjusted to 1T fracture toughness data of F82H plate relative to its master curve and 5% and 95% tolerance bounds.

The first observation of these data is that this material exhibited a very high scatter of fracture toughness data in the transition region. As a reminder, the master curve concept has been originally developed for low-alloy reactor pressure vessel (RPV) steels, and it was anticipated that this methodology would be applicable to cleavage fracture toughness in the transition region for any homogeneous bcc alloys. An example of application of the master curve to fracture toughness data of a variety of RPV steels is given in Figure 2 (Sokolov [2]). Despite the large number of materials, specimens, and irradiation conditions, the master curve provides a very good description of such a large database. In the present study, however, there were only two sizes of specimens of one material, and scatter of fracture toughness data is much larger than for the large RPV data set. For example, at -20°C measured fracture toughness values of F82H varied from 84 to 497 MPa√m. However, the scatter of fracture toughness exhibited by larger and smaller specimens appears to be the same. The characteristic feature of these data is that the upper bound of fracture toughness is increasing with temperature as one would expect for the transition region behavior. At the same time, data on the lower bound of scatter band tend to show increase in the temperature range from -165°C to -100°C. After -100°C, data on the lower bound of scatter tend to level off at about 90 MPa√m level regardless of test temperature. Moreover, at -100°C the data distributed evenly within the scatter band. As temperature increases, data tend to separate in two sub-sets. One sub-set of data follows the master curve trend and another sub-set stays at the lower bound of scatter. This behavior is such that if it might be two mechanisms controlling the fracture of this material. One mechanism would be of the shelf-like nature that might have weak temperature dependence and begin to operate at about 90 MPa√m. And another mechanism would be of a statistical nature (Wallin [3]) and would produce data following the master curve trend.

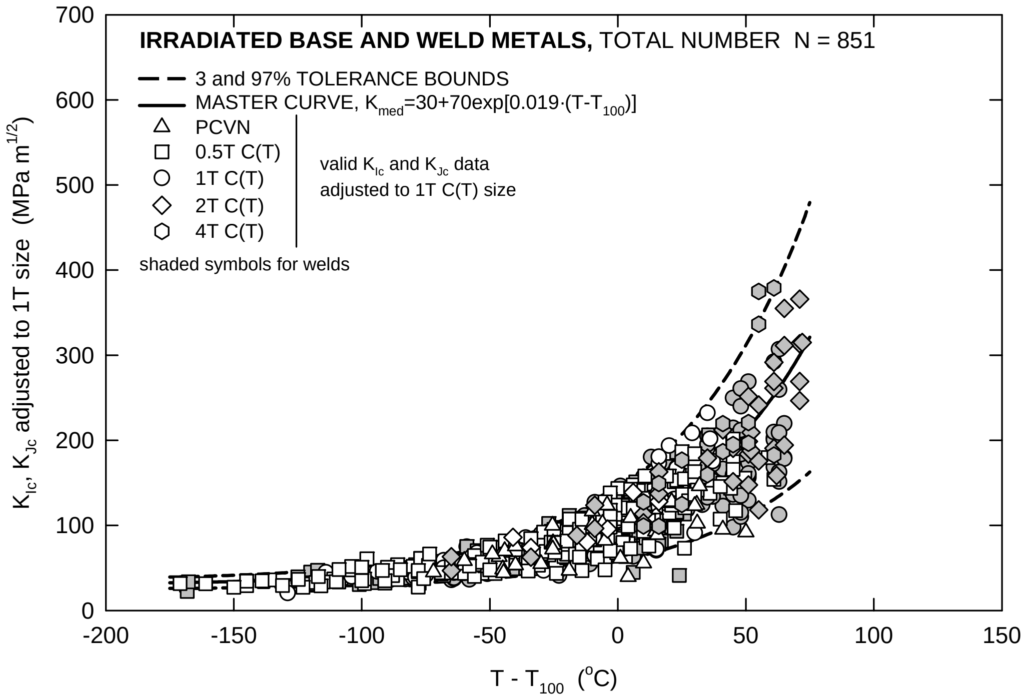

Figure 2: Fracture toughness of large number of RPV steels plotted against reference temperature, T- T_o, relative to the master curve from Ref. [2].

Extensive scanning electro-microscopy has been performed to examine the fractured surfaces of the broken specimens. SEM fractography did not reveal differences in morphology of initiation sites between specimens exhibited high or low fracture toughness values. All specimens failed by cleavage; no evidence of intergranular fracture (IGF) was observed on fractured surfaces. However, the majority of specimens had small regions of intergranular separation on fatigue-precracked portions of broken surfaces. It remains unclear how intergranular separation on fatigue-precracked portions of broken surfaces would have an effect on initiation fracture toughness, since there was no evidence of IGF on fractured surfaces.

5 Summary

A large number of compact specimens of ferretic-martensitic steel F82H was tested in the transition region. The master curve methodology was applied to analyze the data. It was shown that this material exhibited a very large scatter of fracture toughness data in the transition region. The scatter of fracture toughness exhibited by larger and smaller specimens appears to be the same. The scatter of fracture toughness of this material was higher than predicted by master curve 5% and 95% tolerance bonds, and higher than exhibited by a large number of RPV steels. SEM did not reveal differences in morphology between the initiation sites of specimens with high or low fracture toughness.

6 References

[1] Nanstad R.K., Alexander D.J., Swain R.L., Hutton J.T., and Thomas D.L., “A Computer Controlled Automated Test System for Fatigue and Fracture Testing,” in Applications of

Automation Technology for Fatigue and Fracture Testing, ASTM STP 1092, A.A. Braun, N.E. Ashbaugh, and F.M. Smith, Eds., ASTM Philadelphia, 1990, pp. 7-20.
[2] Sokolov M.A. and Nanstad R.K., "Comparison of Irradiation-Induced shifts of K_{Jc} and Charpy Impact Toughness for Reactor Pressure Vessel Steels," Effects of Radiation on Materials: 18th International Symposium, ASTM STP 1325, R.K. Nanstad, M.L. Hamilton, F.A. Garner, and A.S. Kumar, Eds., American Society for Testing and Materials, Philadelphia, 1999, pp. 167-190.
[3] Wallin K., "A Simple Theoretical Charpy-V-KIc Correlation for Irradiation Embrittlement," in Proc. ASME Pressure Vessels and Piping Conference, Innovative Approaches to Irradiation Damage and Fracture Analysis, PVP-Vol. 170, American Society of Mechanical Engineers, New York, pp. 93-100, 1989.